Electrochemical performance of Mo doped high voltage spinel cathode material for lithium-ion battery

T. Kazda[a,*], J. Vondrák[a], A. Visintin[b], M. Sedlaříková[a], J. Tichý[a], P. Čudek[a]

[a] Department of Electrical and Electronic Technology, Faculty of Electrical Engineering and Communication, Brno University of Technology, Technická 10, 616 00, Brno, Czech Republic
[b] Instituto de Investigaciones Fisicoquímicas Teóricas y Aplicadas (INIFTA), UNLP, CCT La Plata-CONICET, CC 16, Suc. 4, CP 1900, La Plata, Argentina

A B S T R A C T

This article deals with the properties of high-voltage cathode material $LiNi_{0.5}Mn_{1.5}O_4$ synthesized by a solid-state reaction method and the influence of doping this material by molybdenum. The samples – $LiMo_{x+y}Ni_{0.5-x}Mn_{1.5-y}O_4$ with different Mo contents ($x = 0.00, 0.05, y = 0.00, 0.05$) were successfully synthesized by two step annealing process and they were then investigated by SEM, EDS spectroscopy, thermo gravimetric analysis, cyclic voltammetry and charge–discharge tests at different loads and high temperature in lithium-ion cells with metal lithium as a counter electrode. Results showed that the initial discharge capacity and capacity during high temperature cycling of the $LiMo_{x+y}Ni_{0.5-x}Mn_{1.5-y}O_4$ cathode were improved with addition of Mo when x = 0.05. Thermal analysis results suggested that the Mo doping slightly improved the stability of the crystal structure of the $LiNi_{0.5}Mn_{1.5}O_4$ cathode which leads to an improved stability during high temperature galvanostatic cycling.

© 2017 Elsevier Ltd. All rights reserved.

1. Introduction

Researchers focused their interest toward modifications of existing cathode materials in order to improve their parameters as a result of searching for new types of cathode materials which could replace currently used cathode materials and allow resolving problems related to the requirements of increasingly higher demand for electrical energy storage particularly in the field of electric vehicles. The result of one of those efforts was the discovery of the cathode material $LiNi_{0.5}Mn_{1.5}O_4$ [1–3]. This material is based on the cathode material $LiMn_2O_4$ in which manganese was partially replaced by nickel. This replacement makes possible charging of the cathode material to 5 V [2,4]. $LiNi_{0.5}Mn_{1.5}O_4$ spinel is same like $LiMn_2O_4$. There are two kinds of crystalline structures depending on the method of synthesis of this material: face centered cubic (Fd3m), referred in the literature as disordered and simple cubic ($P4_332$), referred in the literature as ordered [4–6]. The $LiNi_{0.5}Mn_{1.5}O_4$ material suffers with the same problem as $LiMn_2O_4$ – dissolution of manganese into the electrolyte during cycling at higher temperatures which leads to defects in the structure and capacity decrease [4,7–9]. If we take into account the

high theoretical capacity of this material (148 mAh/g) and its high potential against lithium (∼4.7 V) we get the gravimetric energy density approaching 700 Wh/kg which is approximately 20% more than gravimetric energy density of $LiCoO_2$ and about 30% more than in the case of the cathode material $LiFePO_4$ [8,10]. This cathode material is stable during long term cycling and exhibits good stability at higher current loads because of the spinel structure. These properties make this material interesting for example for use in electric vehicles. This cathode material reaches the high voltage using several oxidation steps at which there occur conversions $LiNi_{0.5}^{II}Mn_{1.5}^{III}O_4/Ni_{0.5}^{IV}Mn_{1.5}^{IV}O_4$. Mn^{3+} oxidizes to Mn^{4+} at 4 V vs Li and Ni^{2+} is subsequently oxidized to Ni^{3+} at the voltage range 4.7–4.8 V vs Li and then to Ni^{4+}. The result of these successive changes of valence of nickel is merging of two discharge plateaus in one very stable discharge plateau [2,4,5,11]. There is the possibility of doping of $LiNi_{0.5}Mn_{1.5}O_4$ with other of other metals to solve the problem of this material with instability at high temperatures. Several different materials were already used for doping, e.g. copper. The amount of doped Cu affects the lattice parameter, lattice configuration, morphology of particles and electrochemical properties. The added copper participates in the electrochemical reaction during charging/discharging thanks to the change in valence of Cu^{+2} to Cu^{+3} [4,12]. The reversible capacity decreases with the increasing amount of Cu but proper optimization of the ratio can improve stability at high loads. E.g. the

material $LiCu_{0.25}Ni_{0.25}Mn_{1.5}O_4$ is due to doping more conductive and the electrochemical properties of this material are consequently enhanced [4]. Another option that has been tested was doping by ruthenium. The materials $LiNi_{0.5}Mn_{1.5}O_4$, $Li_{1.1}Ni_{0.35}Ru_{0.05}Mn_{1.5}O_4$ and $LiNi_{0.4}Ru_{0.05}Mn_{1.5}O_4$ were compared. It has been found, by EIS measurement, that the conductivity rises which leads to the increase of capacity despite of a small part of the active Ni being replaced by Ru [13]. Doping by Cr was also tested, a partial replacement of Ni by Cr occurred in this case. The ionic radius of Cr^{+3} is 0.615 Å which is close to the ion radius of Ni^{+2} (0.65 Å). Partial substitution, such as $LiNi_{0.45}Cr_{0.05}Mn_{1.5}O_4$, leads to improved electrochemical properties due to higher bond strength of the Cr—O bond than in the case of the bonds Ni—O and Mn—O. The stronger Cr—O bond leads to an increase of the rigidity of the material structure and maintaining the properties during long term cycling at higher loads and higher temperatures. Another advantage is that chromium participates in the reaction and the change of valence of Cr^{+3} to Cr^{+4} and back takes place during cycling which leads to the shift of potential of the discharging plateau to 4.8 V against Li [14–16]. A similar phenomenon also occurs during the doping of the material by Al. The ionic radius of Al^{3+} is 0.62 Å and similarly the capacity during cycling at higher loads is stable thanks to the strong Al—O bond [17]. Other elements that have been studied with the aim to improve the properties of the material $LiNi_{0.5}Mn_{1.5}O_4$ were e.g. Fe [18], Co [19], Ti [20], Mg [21], Rh [22] and W [23] .

2. Experimental

The method of reaction in solid state was chosen for the production of this material. Precursors based on carbonates and oxides were chosen as basic materials for the production. Li_2CO_3 (Lithium(II) carbonate), $MnCO_3$ (Manganese carbonate), NiO (Nickel oxide) and MoO_2 (Molybdenum(IV) oxide) were chosen in our case; these materials were mixed in a stechiometric ratio of 0.02 mol/l. The two-step annealing process was selected for the preparation. Selected precursors are milled together in the ball mill FRITSCH Pulverisette 0 for 4 h during the first step of this process. In the first annealing step, the resultant mixture is annealed at 600 °C for 10 h. The second step is annealing at 900 °C for 15 h [24]. After this synthesis, we obtain materials with face-centered spinel structure therefore known as disordered. The prepared material was then mixed into a mixture consisting of NMP (*N*-Methyl-2-pyrrolidon) (solvent), PVDF (Polyvinylidenfluorid) (binder) and carbon Super P. The weight ratio of the materials was: active material 80%, Super P 10%, PVDF 10%. The resulting mixture was subsequently deposited on an Al foil, dried and pressed by the pressure of 3200 kg/cm². A disk with a diameter of 18 mm was cut out of the coated aluminium foil and inserted into the electrochemical test cell El-Cell© ECC-STD. The assembly was done in a

glove box filled with argon atmosphere. Metal Lithium was used as a material for the anode and electrolyte was soaked in a glass fibre separator. 1.5 mol/l $LiPF_6$ EC:DMC 1:2 *w/w* was used as electrolyte.

Cyclic voltammetry and galvanostatic cycling were used for electrochemical characterisation. Cyclic voltammetry was done in the potential window from 3.0 to 5.1 V versus lithium and the scan rate was set to 0.5 mV/s. Galvanostatic cycling was carried out with the same potential window from 3.0 to 5.1 V versus lithium. Two charging and discharging cycles were carried out each time during which the used charging and discharging currents were set to 60 mA/g (related to the weight of the active mass). The real capacity value of the sample was deducted from these two cycles and the sample was then exposed to long term cycling during which it was cycled twenty times by 0.5C current. It was subsequently cycled five times by 1C current, then five times by 2C and then five times by 5C. The next step was cycling again five times by 2C current, again five times by 1C, again ten times by 0.5C and finally there were ten cycles by 0.5C current at the temperature of 50 °C. An assembly consisting of a SEM microscope TESCAN VEGA3 XMU and a Bruker EDAX analyser was used to determine the distribution of elements in the materials. TGA (Thermogravimetric analysis) was used for comparison of thermal stability of the doped cathode materials.

3. Results and discussion

We can see the structure of the samples $LiNi_{0.5}Mn_{1.5}O_4$, $LiMo_{0.05}Ni_{0.45}Mn_{1.5}O_4$ and $LiMo_{0.1}Ni_{0.45}Mn_{1.45}O_4$ after synthesis displayed by SEM in Fig. 1. We can see the structure of the cathode material $LiNi_{0.5}Mn_{1.5}O_4$ after synthesis in Fig. 1A). Used field of view is the same as for other SEM Pictures – 20.8 μm. As we can see there are aggregates of small crystals in the entire volume. The size of the crystals is smaller than 5 μm. SEM analysis of the $LiMo_{0.05}Ni_{0.45}Mn_{1.5}O_4$ cathode material sample is displayed in Fig. 1B). It is clearly evident from the figure that the crystals are interconnected and their size is comparable with the size of crystals of the pristine cathode material $LiNi_{0.5}Mn_{1.5}O_4$. We can see SEM picture of the cathode material $LiMo_{0.1}Ni_{0.45}Mn_{1.45}O_4$ in Fig. 1C); the structure is, in comparison with the two previous samples, different and facets of the crystals are not clearly visible. However, the size of separate particles is approximately similar as the size of particles in the two previous samples (less than 5 μm).

EDS (Energy-dispersive X-ray spectroscopy) analysis with surface mapping of the sample was performed together with the SEM analysis. The EDS spectrum of the samples $LiNi_{0.5}Mn_{1.5}O_4$, $LiMo_{0.05}Ni_{0.45}Mn_{1.5}O_4$ can be seen in Fig. 2. We can see the EDS spectrum obtained from a sample of the cathode material $LiNi_{0.5}Mn_{1.5}O_4$ in Fig. 2A). It is evident from the recorded spectra that the material contains all estimated elements (Ni, Mn, and O). The EDS spectrum obtained from a sample of the cathode material
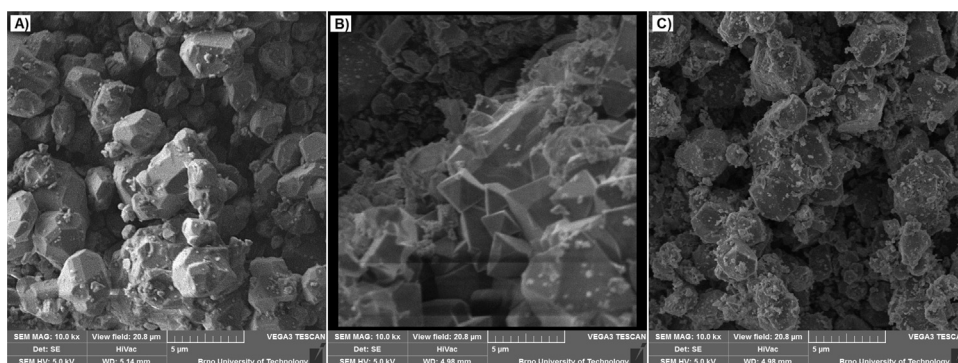

Fig. 1. SEM analysis of the samples A) $LiNi_{0.5}Mn_{1.5}O_4$, B) $LiMo_{0.05}Ni_{0.45}Mn_{1.5}O_4$ and C) $LiMo_{0.1}Ni_{0.45}Mn_{1.45}O_4$; used view field: 20.8 μm.